Chemical Science

Accepted Manuscript

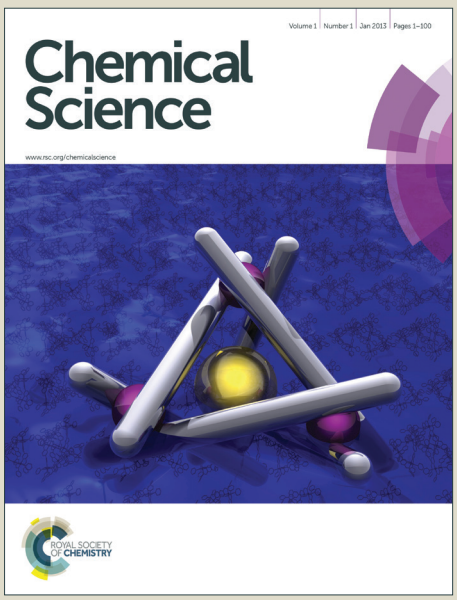

ROYAL SOCIETY OF CHEMISTRY

www.rsc.org/chemicalscience

Chemical Science

RSCPublishing

EDGE ARTICLE

A macrocycle-assisted nanoparticlization process for bulk Ag_2S †‡

Cite this: DOI: 10.1039/x0xx00000x

Xin He,[a] Yuechao Wang,[b] Cai-Yan Gao,[a] Hong Jiang[b] and Liang Zhao*[a]

Received 00th January 2012,
Accepted 00th January 2012

DOI: 10.1039/x0xx00000x

www.rsc.org/

We report herein a new nanoparticlization process for the bulk-to-nano transformation of Ag_2S by incorporating both top-down and bottom-up approaches. Bulk Ag_2S was dissolved in solution with the assistance of a macrocyclic ligand hexamethylazacalix[6]pyridine **Py[6]** to produce polynuclear silver sulfide cluster aggregates. All Ag-S cluster aggregates obtained in three crystalline complexes were protected by **Py[6]** macrocycles. Removing the protective **Py[6]** macrocycles by protonation led to the generation of unconventional Ag-S nanoparticles with a large gap energy. Theoretical calculation by hybrid DFT method demonstrated that the silver-sulfide clusters with high Ag/S ratio exhibited more localized HOMO-LUMO orbitals, which consequently enlarged their band gap energies. These experimental and theoretical studies broaden our comprehension on the fabrication of nanomaterials by virtue of the advantages of both bottom-up and top-down methods and meanwhile provide a viable means of adjusting the band gap of binary nanomaterials independent of their size.

Introduction

Silver sulfide, a type of direct and well-known narrow band gap semiconductor,[1] has attracted considerable attention due to its good stability, low toxicity[2] and extensive potential applications in photovoltaic cells, photoconductors,[3] infrared detectors[4] and near-infrared imaging.[5] Besides a band gap of 0.9-1.1 eV for bulk α-Ag_2S,[6] diminishing the size of Ag_2S to a nano-sized scale provides an efficient way to finely tune the band gap of this material based on the quantum confinement effect, thus resulting in many intriguing size-specific optical and optoelectronic properties.[7] In this regard, different synthetic methods[6] *e.g.* microemulsion approach,[8] hot injection method[9] etc. have been comprehensively explored during the past two decades with an aim at achieving uniformly sized Ag_2S nanocrystals. However, the use of exotic ligand- or surfactant-stabilized silver and sulfide ions or their precursors and the requirement of elevated temperature and high pressure in most cases made these methods an arduous synthetic protocol. Obviously, if bulk Ag_2S solid can be directly transformed into its nano-sized prototype, it will be a concise and ideal synthetic strategy. However, to the best of our knowledge, no reported method for the synthesis of silver chalcogenide nanomaterials involves such kind of direct transformation.

Recently, the synthesis of silver chalcogenide nanocluster compounds in crystalline form has been reported in literatures.[10,11] During the reaction between various silver thiolates (SR) and silylated sulfide sources in the presence of coordinative phosphane ligands, nanometer-sized Ag/S/SR silver clusters can be generated at room temperature, but amorphous Ag_2S would be obtained if increasing the reaction temperature. Such biased reaction pathways suggest a possible intermediate role of silver-sulfide clusters in the synthesis of silver sulfide nano-objects. Inspired by this understanding, we envision that successful transformation of bulk Ag_2S to silver sulfide nanomaterials could be initiated with the synthesis of polynuclear silver sulfide cluster directly from bulk Ag_2S. Combination of top-down (from bulk Ag_2S to silver sulfide clusters) and bottom-up (from silver sulfide clusters to nanomaterials) approaches may facilitate the bulk-to-nano transformation of Ag_2S. However, bulk Ag_2S is known for its very poor solubility (K_{sp} = 8*10^{-51} at 25 ºC), which makes it a formidable challenge to dissolve bulk Ag_2S solid and complete the bulk-to-nano transformation by means of cluster intermediates. Very recently, we explored that a new class of

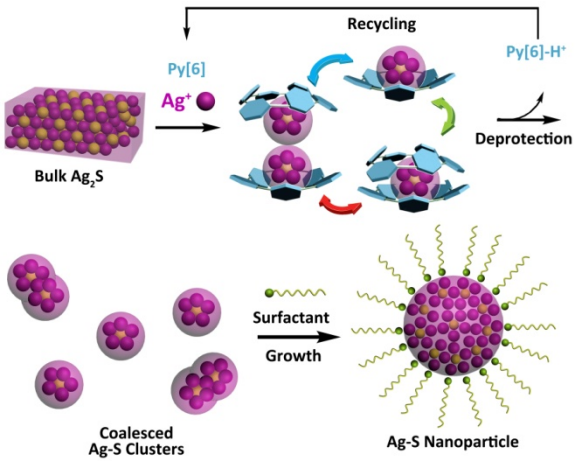

Scheme 1 Macrocycle-assisted bulk-to-nano transformation of Ag_2S.

macrocycles, azacalix[*n*]pyridines (**Py[*n*]**), exhibited a positive allosteric effect upon binding with metal ions,[12] which largely enhanced their affinity to a multimetallic aggregate and led to the formation of silver acetylide clusters by using slightly soluble polymeric $[RC{\equiv}CAg]_n$ as starting materials.[13] We thus conceive a synthetic strategy to implement the bulk-to-nano transformation of silver sulfide as illustrated in Scheme 1. A particular polypyridine macrocyclic ligand **Py[*n*]** will be used to facilitate the formation of macrocycle-protected silver sulfide clusters based on its positive allosteric effect at first. Upon interrupting coordination bonds between polypyridine ligands and silver atoms via protonation, the encapsulated silver sulfide clusters may mutually coalesce to finally produce silver sulfide nanoparticles, which can be stabilized by additional surfactants.

Results and discussion

Considering the high efficiency of **Py[6]** (composed of six 1,3-pyridine rings bridged by six N-CH_3 moieties)[14] in our previous synthesis of silver ethynediide cluster-encapsulated supramolecular capsule,[13b] we firstly attempted to utilize this macrocyclic ligand to dissolve Ag_2S solid. When Ag_2S solid was added into a methanol solution of $AgCF_3SO_3$ (0.2M), no obvious color change of the solution was observed. However, addition of **Py[6]** into the Ag_2S-$AgCF_3SO_3$ mixture led to the appearance of yellow color very quickly and the gradual decrease of the Ag_2S solid, suggesting the dissolution of Ag_2S into the solution. It should be noticed that silver triflate is essential for dissolving Ag_2S solid since only mixing Ag_2S with **Py[6]** cannot cause any color change. We next carried out the ^{1}H-NMR analysis of the reaction mixture of Ag_2S-$AgCF_3SO_3$-**Py[6]**. In the ^{1}H-NMR spectrum, there were three triplet peaks at 8.05 (Ha), 7.87 (Hb) and 7.60 (Hc) ppm corresponding to the pyridyl γ-protons of **Py[6]** (Fig. 1a). Typical downfield shift of these peaks relative to the neat **Py[6]** (7.46 ppm for pyridyl γ-protons)[14] suggested the occurrence of coordination between **Py[6]** and silver ions. Furthermore, diffusion ordered spectroscopy (DOSY) exhibited two diffusion bands (Fig. 1b), implying the existence of two dominant assembled species in the reaction mixture. As shown in Figure 1b, the species

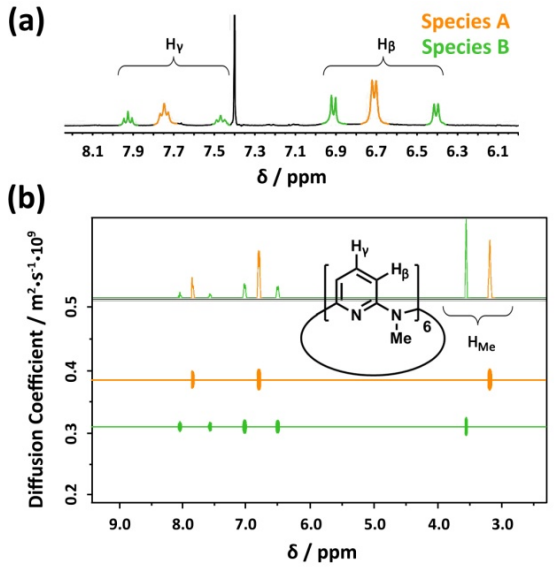

Fig. 1 (a) Partial ^{1}H NMR spectrum (400 MHz, $CDCl_3$:methanol-D_4 (v:v) = 1:1, 25.0 ºC) and b) DOSY spectrum of the reaction mixture of $AgCF_3SO_3$, Ag_2S and **Py[6]**.

to the signal Hb (denoted as **A**) has a larger diffusion coefficient than another species (denoted as **B**) accounting for the signals Ha and Hc. The diameter ratio of **A** to **B** in classical spherical model was deduced as 0.80 based on their respective diffusion coefficients and the Stokes-Einstein equation, which agrees quite well with the ratio (0.78) of the measured distances between the two most separated points of the functional units in the crystal structures of **1** and **2** *vide infra*.

The NMR titration experiment of **Py[6]** with silver triflate clarified that the species **A** was actually derived from the assembly of silver triflate and **Py[6]** due to identical proton NMR spectra (see Fig. S1 in the Supporting Information). Single crystals of the species **A** (denoted as crystalline complex **1**) for X-ray crystallography analysis were deposited from the CH_3OH/CH_2Cl_2 mixed solution of **Py[6]** and $AgCF_3SO_3$. As shown in Fig. 2a, the ratio of silver triflate to **Py[6]** in complex **1** was determined as 3:1, giving the formula of **1** as $\{Ag_3(\mathbf{Py[6]})(CF_3SO_3)_3(H_2O)_{0.5}\}$. A central silver atom Ag1 in **1** adopted a linear coordination geometry to bind with two opposite pyridines of the **Py[6]**, thus causing the formation of a cage-like structure. This unimolecular folding fashion is similar with our previously reported scenarios for two larger macrocycles **Py[8]** and **Py[9]**.[12]

The structural analysis of the species **B** was complicated. High-resolution mass spectroscopy (HR-MS) of the Ag_2S-$AgCF_3SO_3$-**Py[6]** yellow reaction mixture revealed two isotopically well-resolved peaks at m/z = 1258.9341 and 554.9862 corresponding to the $[(CF_3SO_3)_2Ag_3(\mathbf{Py[6]})]^+$ and $[(CF_3SO_3)Ag_3(\mathbf{Py[6]})]^{2+}$ species (Fig. S2), confirming the existence of the species **A**. In addition, several peaks corresponding to the species composed of a **Py[6]** macrocycle and a polynuclear silver-sulfide cluster plus some silver triflate groups have been found as well in HR-MS (Fig. S2). For example, a strong peak at m/z = 1762.5754 can be ascribed to the species $[Ag_6S(\mathbf{Py[6]})(CF_3SO_3)_3]^+$ and the peak at m/z = 934.7313 is isotopically in good agreement with the species $[Ag_7S(\mathbf{Py[6]})(CF_3SO_3)_3]^{2+}$. We then conducted a crystallization process on this reaction mixture by adding diethyl ether and a crystalline compound with the formula of $[Ag_5S(\mathbf{Py[6]})](CF_3SO_3)_3{\bullet}(CH_3OH)$ (**2**) was finally obtained. Crystal structure of **2** (Fig. 2b) comprises a central sulfur anion that is encompassed by six silver atoms while two of them (Ag5 and Ag6) each has an occupancy ratio of 0.5. This silver-sulfide cluster should be properly described as a $[Ag_5\text{-}S]$ aggregate, which is coordinated by a **Py[6]** macrocycle at one side and is further bonded by three triflate anions at another side. Argentophilic interactions[15] and silver−aromatic π interactions both play a significant role in the stabilization of such a $[Ag_5\text{-}S]$ cluster situated inside a **Py[6]** macrocycle. Interestingly, similar crystallization process but with longer crystallization time than that for complex **2** resulted in a new crystalline complex **3**, which has a formula of $[Ag_5S(\mathbf{Py[6]})_2](CF_3SO_3)_3$ based on its crystal structure analysis. As shown in Fig. 2c, complex **3** also comprises a $[Ag_5\text{-}S]$ aggregate with a C_2-axis symmetry, which is protected by two face-to-face **Py[6]** ligands to construct a cluster-embedded supramolecular capsule. To the best of our knowledge, this is the first example of a discrete silver sulfide cluster with an inner penta-coordinated sulfide.[16] This $[Ag_5\text{-}S]$ structural motif is also consistent with the basic structural unit of bulk Ag_2S.[17] But in contrast, the Ag-S bond lengths in **3** (2.369(3)-2.432(4) Å) are ~0.2 Å shorter than the values in the bulk Ag_2S[17] and other silver-sulfide clusters.[11,16,18] Another crystalline complex $[Ag_{12}S_2(\mathbf{Py[6]})_2](CF_3SO_3)_8{\bullet}H_2O{\bullet}CH_3OH$ (**4**) was serendipitously acquired upon reducing the amount of **Py[6]** applied in the above synthetic procedure for complex **2**. As shown in Fig. 2d, the dumbbell-shaped $[Ag_{12}S_2]$ silver-sulfide cluster aggregate in **4** can be described as two single sulfide-centered cage-

like silver clusters fused by sharing a middle silver atom. In addition, the upper and nether sides of this dumbbell-shaped silver cluster were emboweled by two **Py[6]** macrocycles as similar as in **3**. The total seven silver atoms in the asymmetric unit of **4** shared a refined site occupancy of six since silver atom Ag6 was located at a special symmetry position while Ag7 is disordered and both had a refined site-occupancy ratio less than one (see Supporting Information for details). Despite of structural difference of silver-sulfide clusters among complexes **2-4** both in nuclearity number and cluster configuration, the **Py[6]** macrocycles in **2-4** all adopted a similar quasi-C_{3v} bowl-shaped conformation. Moreover, we substaniated that most silver-sulfide cluster species in the reaction mixture of Ag_2S, $AgCF_3SO_3$ and **Py[6]** were stabilized by one or two **Py[6]** macrocyclic ligands. In addition, based on the HR-MS, ^{1}H-NMR data and the DOSY result that reflected a size ratio (0.80) comparable to the value of 0.78 in the crystal structures of **1** and **2**, we hypothesized that complex **2** that composed of a **Py[6]** macrocycle and a polynuclear silver-sulfide cluster is probably the second dominant species (the species **B)** in the reaction mixture of Ag_2S, $AgCF_3SO_3$ and **Py[6]**.

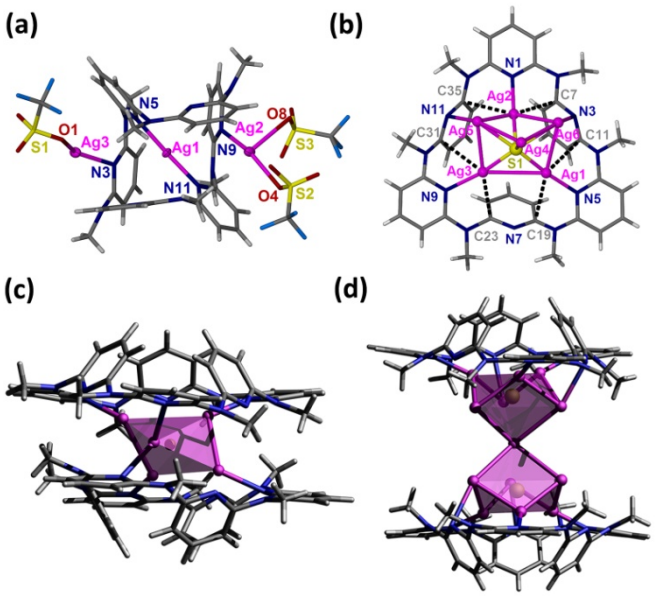

Fig. 2 (a) Crystal structure of complex $\{Ag_3(\mathbf{Py[6]})(CF_3SO_3)_3(H_2O)_{0.5}\}$ (**1**). Selected bond distances (Å): Ag1-N5 2.154(3); Ag1-N11 2.168(3); Ag2-N9 2.281(4); Ag3-N3 2.284(3). (b) Partial crystal structure of $[Ag_5S(\mathbf{Py[6]})](CF_3SO_3)_3\bullet CH_3OH$ (**2**). Ag5 and Ag6 each has an occupancy ratio of 0.5. The three triflate groups at top side of the [Ag5-S] cluster were omitted for clarity. Silver-aromatic π interactions were shown by dashed lines. Ag-C distances (Å): Ag1-C11 2.987; Ag1-C19 2.948; Ag2-C7 2.731; Ag2-C35 2.957; Ag3-C23 2.836; Ag3-C31 3.090. (c) Side view of complex $[Ag_5S(\mathbf{Py[6]})_2](CF_3SO_3)_3$ (**3**) with the central silver-sulfide cluster presented by a polyhedron. (d) Crystal structure of $[Ag_{12}S_2(\mathbf{Py[6]})_2](CF_3SO_3)_8\bullet H_2O\bullet CH_3OH$ (**4**). Two silver atoms each has an occupancy ratio of 0.5. Triflate groups and solvent molecules were omitted for clarity. Color scheme for atoms: Ag, purple; C, gray; H, white; N, blue; S, yellow; F, cyan.

Successful isolation of discrete (in **2** and **3**) and joint (in **4**) silver sulfide clusters by varying the amount of the protective **Py[6]** proves the viability of synthesizing Ag-S binary nanoparticles through the coalescence and fusion of silver sulfide clusters. In view of the fact that **Py[6]** can be easily protonated by a strong acid due to the good Lewis basicity of pyridine, we then added CF_3COOH into the filtrate of the reaction mixture of Ag_2S, $AgCF_3SO_3$ and **Py[6]** to interrupt the coordination interactions between the central silver sulfide cluster and its surrounding **Py[6]** macrocycles. Dismantlement of **Py[6]** led to a clear yellow solution. This solution sample remained its yellow color within an hour, but further standing would result in a black precipitate. Formation and stepwise growth of metal sulfide nanoparticles were affirmed by transmission electron microscopy (TEM) photographs prepared at different intervals (Fig. 3a-b). We subsequently employed oleic amine[9] as a surfactant to stabilize the acquired nanoparticles. The resulting yellow solution can retain its solution homogeneity for several days. TEM images of this solution sample (denoted as **D-NP**) substantiated the formation of metal nanoparticles with an average diameter of 4±0.4 nm (Fig. 3c). Fourier transform IR spectroscopy analysis of the solid sample of **D-NP** prepared by centrifugation clearly showed the absence of **Py[6]** and the existence of oleic amine molecules in **D-NP** (Fig. S3). This observation verified our above assumption that **Py[6]**-protected silver sulfide clusters could indeed undergo a deprotection process to act as nuclei and activated monomers for the fabrication of silver sulfide nanoparticles. Notably, we found that the acidified **Py[6]** ligands can be recycled after neutralization and extraction and then employed for subsequent bulk-to-nano transformation of silver sulfide.

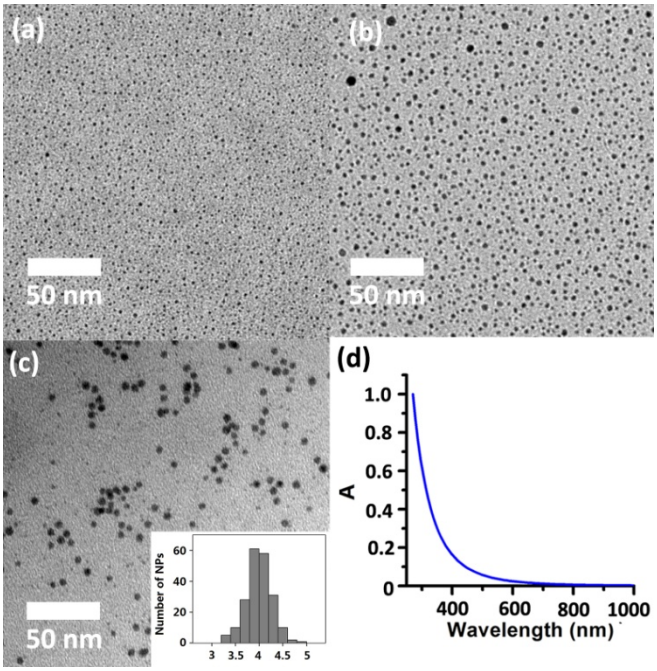

Fig. 3 TEM images of deprotected silver sulfide clusters after adding CF_3COOH (a) 30 s and (b) 2 min later. (c) TEM images of sample **D-NP**. (inset) Size-distribution histogram of silver sulfide nanoparticles in **D-NP**. (d) UV-vis spectrum of **D-NP** in cyclohexane at 298 K.

On the other hand, high-resolution TEM (HR-TEM) of **D-NP** showed very ambiguous lattice fringes in contrast to the clear pattern in previously reported Ag_2S nanoclusters,[19] suggesting a poorly crystalline form of **D-NP**. The low crystallinity of **D-NP** was further substantiated by selected area electron diffraction (SAED) (Fig. S4), which exhibited two feeble diffraction rings that could be indexed to the (-103) and (232) facets of monoclinic Ag_2S (JCPDS card 14-0072). The

energy dispersive X-ray spectroscopy (EDX) of **D-NP** indicated the presence of element Ag and S and further offered the Ag/S atomic ratio equaling to 3.5 (Fig. S5). We also conducted the XPS experiment of **D-NP**. As reflected in the XPS experiment (Fig. S6), we confirmed the +1 oxidation state of the silver atoms in **D-NP** based on their Ag $3d^{5/2}$ and Ag $3d^{3/2}$ binding energy peaks at 374.5 and 368.5 eV. In addition, the Ag/S molar ratio was determined as 3.7 based on the XPS data, which is comparable to the energy dispersive X-ray spectroscopy (EDX) data of 3.5. This Ag/S elemental ratio in **D-NP** is larger than the values of around 2.0 in bulk Ag_2S[17] and previously reported silver sulfide nanoclusters.[1,3,19] We hypothesized that such high Ag/S ratio in **D-NP** may arise from the coalescence and fusion of the silver-rich Ag-S clusters in **2-4** by forming inter-cluster interactions (e.g., argentophilicity) and sharing silver atoms as similar as the above-mentioned scenarios in **2-4**. In addition, the absorption spectrum of the cyclohexane solution of **D-NP** (Fig. 3d) exhibited a monotonic decrease in the whole recorded range, which is similar to the spectra of a number of reported silver sulfide nanocluster samples.[20] The band gap energy could be fitted by using the Bardeen or Tauc equation (Fig. S7). Direct transitions of **D-NP** was thus deducted to be 4.0 eV, largely blue-shifting relative to the band gap of the bulk α-Ag_2S.[6] It is noteworthy that modifying the composition ratio of different constituents in nanomaterials in order to perform band gap adjustment has been frequently applied in ternary and quaternary alloyed semiconductor nanomaterials, but rarely in binary systems.[21] The method reported herein represents a viable means to tune the band gap of binary nanomaterials independent of their size.

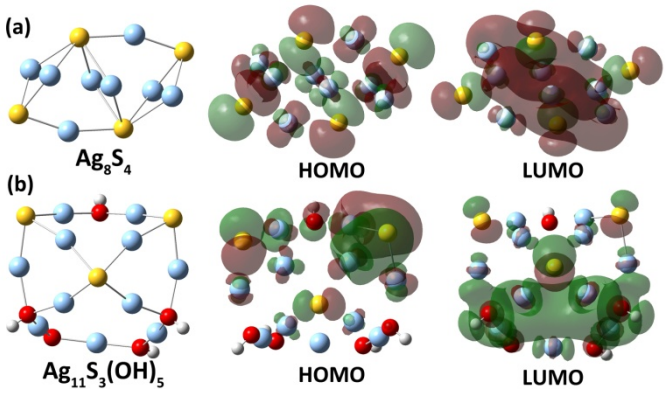

Fig. 4 Optimized structures of two Ag-S clusters (a) Ag_8S_4 and (b) $Ag_{11}S_3(OH)_5$ with different Ag/S elemental ratios and their HOMO and LUMO orbitals.

In order to make clear the relationship between the gap energy and the Ag/S ratio in silver sulfide clusters, we embarked on a theoretical HOMO-LUMO gap calculation of silver sulfide clusters with different Ag/S ratios via hybrid density functional theory (DFT) method (see calculation details in the Supporting Information). It is highly challenging and exceedingly difficult to construct a structural model and optimize the structure of a 4 nm Ag-S cluster. We thus carried out calculation on four small Ag-S clusters (Ag_8S_4, $Ag_{10}S_5$, $Ag_{11}S_3(OH)_5$ and $Ag_{12}S_3(OH)_6$) with different Ag:S ratios (Figure 4). The initial structures of the four clusters were built up according to the reported structural motifs of α-Ag_2S[22] and crystal structures of silver sulfide clusters.[10-11] For the sake of simplifying the structural optimization and energy gap computation, hydroxyl groups were used as the substitution of the coordinated peripheral $CF_3SO_3^-$ and $CF_3CO_2^-$ anions in the calculation of silver sulfide clusters with the Ag/S ratio larger than two. As reflected in the calculated results (Table S1), the two clusters Ag_8S_4 and $Ag_{10}S_5$ with the Ag/S ratio of two have a HOMO-LUMO gap energy of 2.45 and 1.86 eV, respectively. In contrast, the other two size-comparable clusters $Ag_{11}S_3(OH)_5$ and $Ag_{12}S_3(OH)_6$ with the Ag/S ratio larger than 2 have a corresponding gap energy of 3.11 and 3.09 eV. This calculated results agreed well with the trend in our above experiment. Compared with the two clusters Ag_8S_4 and $Ag_{10}S_5$, $Ag_{11}S_3(OH)_5$ and $Ag_{12}S_3(OH)_6$ with higher Ag:S elemental ratio exhibited more localized HOMO-LUMO orbitals (Fig. 4 and Fig. S8). Less dispersed orbitals in these two Ag-S clusters ultimately led to the band gap enlargement.

Conclusions

In summary, we have demonstrated a viable means of synthesizing silver sulfide nanomaterials directly from its bulk form in terms of the assistance of coordinative macrocyclic ligands. This method could be successfully applied in the fabrication of other binary silver nanomaterials such as silver halides, acetylides etc. based on our recent investigation. Considering the size of macrocyclic ligands can dominate the nuclearity number of acquired metal cluster aggregates, this approach can also be employed to achieve nanomaterials with different properties dependent on different nucleation centers. This study foresees the synthesis of numerous new nanomaterials with novel properties based on their synthetic revisiting inspired by the combination of bottom-up and top-down methods reported herein.

Acknowledgements

Financial support by the MOST (973 program, 2013CB834501 and 2011CB932501) and NNSFC (91127006, 21132005, 21121004) is gratefully acknowledged. This work is also supported by MOE (NCET-12-0296), Tsinghua University Initiative Scientific Research Program (2011Z02155) and Beijing Higher Education Young Elite Teacher Project (YETP0130). We are grateful to Profs. Mei-Xiang Wang and De-Xian Wang for their helpful discussion.

Notes and references

[a] The Key Laboratory of Bioorganic Phosphorus Chemistry & Chemical Biology (Ministry of Education), Department of Chemistry, Tsinghua University, Beijing 100084, China. E-mail: zhaolchem@mail.tsinghua.edu.cn.

[b] Beijing National Laboratory for Molecular Sciences, State Key Laboratory of Rare Earth Materials Chemistry and Applications, Institute of Theoretical and Computational Chemistry, College of Chemistry and Molecular Engineering, Peking University, Beijing 100871, China.

† Electronic Supplementary Information (ESI) available: Synthetic procedures and crystal structure determination details. Analytical data, spectra, and images. X-ray crystallographic data for **1-4** in CIF format. See DOI: 10.1039/b000000x/

‡ This work is dedicated to Professor Thomas C. W. Mak in celebration of his 78th birthday.

1 (*a*) K. Akamatsu, S. Takei, M. Mizuhata, A. Kajinami, S. Deki, S. Takeoka, M. Fujii, S. Hayashi and K. Yamamoto, *Thin Solid Films*,

2000, **359**, 55; (*b*) W. P. Lim, Z. Zhang, H. Y. Low and W. S. Chin, *Angew. Chem. Int. Ed.*, 2004, **43**, 5685.

2 P. Hirsch, *Environ. Toxicol. Chem.*, 1998, **17**, 601.

3 (*a*) K. Terabe, T. Hasegawa, T. Nakayama and M. Aono, *Nature*, 2005, **433**, 47; (*b*) F. Gao, Q. Y. Lu and D. Y. Zhao, *Nano Lett.*, 2003, **3**, 85; (*c*) V. M. Huxter, T. Mirkovic, P. S. Nair and G. D. Scholes, *Adv. Mater.*, 2008, **20**, 2439; (*d*) W. J. Lou, X. B. Wang, M. Chen, W. M. Liu and J. C. Hao, *Nanotechnology*, 2008, **19**, 225607; (*e*) J. H. Xiang, H. Q. Cao, Q. Z. Wu, S. C. Zhang, X. R. Zhang and A. A. R. Watt, *J. Phys. Chem. C*, 2008, **112**, 3580; (*f*) Y. Lei, H. Jia, W. He, Y. Zhang, L. Mi, H. Hou, G. Zhu and Z. Zheng, *J. Am. Chem. Soc.*, 2012, **134**, 17392; (*g*) B. Liu, D. Wang, Y. Zhang, H. Fan, Y. Lin, T. Jiang and T. Xie, *Dalton Trans.*, 2013, **42**, 2232; (*h*) P.-J. Wu, J.-W. Yu, H.-J. Chao and J.-Y. Chang, *Chem Mater.*, 2014, **26**, 3485.

4 G. Hodes, J. Manassen and D. Cahen, *Nature*, 1976, **261**, 403.

5 (*a*) Y. Du, B. Xu, T. Fu, M. Cai, F. Li, Y. Zhang and Q. Wang, *J. Am. Chem. Soc.*, 2010, **132**, 1470; (*b*) M. Yarema, S. Pichler, M. Sytnyk, R. Seyrkammer, R. T. Lechner, G. Fritz-Popovski, D. Jarzab, K. Szendrei, R. Resel, O. Korovyanko, M. A. Loi, O. Paris, G. Hesser and W. Heiss, *ACS Nano*, 2011, **5**, 3758; (*c*) G. Hong, J. T. Robinson, Y. Zhang, S. Diao, A. L. Antaris, Q. Wang and H. Dai, *Angew. Chem. Int. Ed.*, 2012, **51**, 9818.

6 S. V. Kershaw, A. S. Susha and A. L. Rogach, *Chem. Soc. Rev.*, 2013, **42**, 3033.

7 (*a*) A. Tubtimtae, K. Wu, H. Tung, M. Lee and G. Wang, *Electrochem. Commun.*, 2010, **12**, 1158; (*b*) R. Wang, R. Tangirala, S. Raoux, J. Jordan-Sweet and D. Milliron, *Adv. Mater.*, 2012, **24**, 99; (*c*) E. Kong, Y. Chang, H. Park and H. Jang, *Small*, 2014, **10**, 1300.

8 (*a*) V. Buschmann, G. Van Tendeloo, P. Monnoyer and J. B. Nagy, *Langmuir*, 1998, **14**, 1528; (*b*) X. Jiang, Y. Xie, J. Lu, L. Zhu, W. He and Y. Qian, *J. Mater. Chem.*, 2001, **11**, 584.

9 D. Wang, T. Xie, Q. Peng and Y. Li, *J. Am. Chem. Soc.*, 2008, **130**, 4016.

10 (*a*) J. F. Corrigan, O. Fuhr and D. Fenske, *Adv. Mater.*, 2009, **21**, 1867; (*b*) O. Fuhr, S. Dehnen and D. Fenske, *Chem. Soc. Rev.*, 2013, **42**, 1871.

11 G. Li, Z. Lei and Q.-M. Wang, *J. Am. Chem. Soc.*, 2010, **132**, 17678.

12 X. He, X.-B. Xu, X. Wang and L. Zhao, *Chem. Commun.*, 2013, *49*, 7153.

13 (a) C.-Y. Gao, L. Zhao and M.-X. Wang, *J. Am. Chem. Soc.*, 2011, **133**, 8448; (b) C.-Y. Gao, L. Zhao and M.-X. Wang, *J. Am. Chem. Soc.*, 2012, **134**, 824; (c) C.-Y. Gao, X. He, L. Zhao and M.-X. Wang, *Chem. Commun.*, 2012, **48**, 8368; (d) X. He, C.-Y. Gao, M.-X. Wang and L. Zhao, *Chem. Commun.*, 2012, **48**, 10877.

14 E.-X. Zhang, D.-X. Wang, Q.-Y. Zheng and M.-X. Wang, *Org. Lett.*, 2008, **10**, 2565.

15 (a) M. Jansen, *Angew. Chem. Int. Ed. Engl.*, 1987, **26**, 1098; (b) P. Pyykkö, *Chem. Rev.*, 1997, **97**, 597.

16 Discrete μ_4-S silver cluster: V. W.-W. Yam, K. K.-W. Lo, C.-R. Wang and K.-K. Cheung, *Inorg. Chem.*, 1996, **35**, 5116.

17 D. Santamaría-Pérez, M. Marqués, R. Chuliá-Jordán, J. M. Menendez, O. Gomis, J. Ruiz-Fuertes, J. A. Sans, D. Errandonea and J. M. Recio, *Inorg. Chem.*, 2012, **51**, 5289.

18 R. Ahlrichs, A. Eichhöfer, D. Fenske, O. Hampe, M. M. Kappes, P. Nava and J. Olkowska-Oetzel, *Angew. Chem. Int. Ed.*, 2004, **43**, 3823.

19 (*a*) A. Sahu, L. Qi, M. S. Kang, D. Deng and D. J. Norris, *J. Am. Chem. Soc.*, 2011, **133**, 6509; (*b*) R. Rica and A. H. Velders, *J. Am. Chem. Soc.*, 2011, **133**, 2875; (*c*) Y. Zhang, Y. Liu, C. Li, X. Chen and Q. Wang, *J. Phys. Chem. C*, 2014, **118**, 4918.

20 (*a*) V. M. Huxter, T. Mirkovic, P. S. Nair and G. D. Scholes, *Adv. Mater.*, 2008, **20**, 2439; (*b*) M. Yarema, S. Pichler, M. Sytnyk, R. Seyrkammer, R. T. Lechner, G. Fritz-Popovski, D. Jarzab, K. Szendrei, R. Resel, O. Korovyanko, M. A. Loi, O. Paris, G. Hesser and W. Heiss, *ACS Nano*, 2011, **5**, 3758.

21 (*a*) J. M. Luther and J. M. Pietryga, *ACS Nano*, 2013, **7**, 1845; (*b*) S. J. Oh, N. E. Berry, J.-H. Choi, E. A. Gaulding, T. Paik, S.-H. Hong, C. B. Murray and C. R. Kagan, *ACS Nano*, 2013, **7**, 2413.

22 D. Santamaría -Pérez, M. Marqués, R. Chuliá-Jordán , J. M. Menendez, O. Gomis, J. Ruiz-Fuertes, J. A. Sans, D. Errandonea, J. M. Recio, *Inorg. Chem.* 2012, **51**, 5289.